FOPID-Based Load Frequency Control of Nonlinear Multi-Area Power Systems via Mayfly Optimization Algorithm

M. Fathy*
Electrical Power and Machines Department
Faculty of Engineering (Shoubra),
Benha University
Cairo, EGYPT
mohamed.fathy@feng.bu.edu.eg

M. Soliman
Electrical Power and Machines Department
Faculty of Engineering (Shoubra),
Benha University
Cairo, EGYPT
mahmoud.halal@feng.bu.edu.eg

***Abstract*—In this paper, design of fractional order proportional-integral-derivative (FOPID) controllers in nonlinear multi-area interconnected systems, is presented. A three-area test system is considered to carry out this study. Typically, each turbine has limited generation rate constrain (GRC), while nonlinear performance of governor is described by its dead band (DB). Time delays imposed by signal telemetry are considered as well. Mayfly optimization algorithm (MOA) is proposed to compute the optimum parameters of FOPIDs, while minimizing a time domain based objective function. The system time response stimulated by step-load perturbation (SLP) is quantized using common ITAE index. The proposed design is compared to other designs optimized using different intelligent algorithms where the superiority of the proposed is emphasized. Robustness test based on Hermite-Biehler theorem showed that system is stable subject to parametric-uncertainties.**

Keywords— LFC; FOPID; Time delay; GRC; Dead band; MOA; Hermite-Biehler theorem.

I. INTRODUCTION

The dynamic balance between power generation and total load demand plus system power losses are essential for load frequency control in power systems. When this balance is disrupted, frequency deviation, change of scheduled power exchange between controlled areas and change of operation point will occur, which in result will lead system to separation and further instability consequences. To preserve system stability, load frequency control (LFC) is used which is defined as the regulation of the power output of generators within a controlled area, LFC changes unit generation by changing operation point to keep the balance between generation and total load demand. Power systems are usually divided into various areas. Each area has its own generation, loads and system losses. Those areas are interconnected through tie lines. The tie lines are utilized for interchange scheduled power between the connected areas and provide inter-area support in case of abnormal conditions. To keep the power interchanges between areas at their scheduled values power system secondary regulation loop which usually called AGC is used. PID, FOPID, PIDA (proportional integral derivative acceleration [1], sliding mode controller (SLMC)[2], [3], fuzzy logic controller (FLC) [4]are some types of controllers which used in AGC. Various comparisons between LFC methodologies are presented in [5]. There are assortment of different computational intelligence-based techniques exist for suitable tuning of the LFCs controller parameters. Many Global optimization techniques as well as computational intelligence-based techniques have been employed in the design of LFCs. Artificial bee colony (ABC) algorithm

Nomenclature

i	subscript referred to area i	T_{ri}	steam turbine reheat time constant of area i (s)
R_i	governor speed regulation parameter of area i (Hz/ p.u. MW)	K_{ri}	steam turbine reheat constant of area i
H_i	Inertia constant of area i (s)	K_{pi}	$1/D_i\,(Hz/p.u.)$
f_i	nominal system frequency (Hz)	T_{sim}	simulation time (s)
Δf_i	incremental change in frequency of area i (Hz)	k_P	gain of proportional controller in area i
ΔP_{tie}	incremental change in tie line power of tie i (p.u.)	k_I	gain of integral controller in area i
D_i	$\Delta P_{Di}/\Delta f_i\,(p.u/Hz)$	k_D	gain of derivative controller in area i
T_{pi}	$2H_i/f_iD_i\,(s)$	λ	The exponential of integral operator
T_{gi}	steam governor time constant of area i (s)	μ	The exponential of the differential operator
T_{ti}	steam turbine time constant of area i (s)	ACE	area control error

Applied to PID controllers in linear single, two and multi-area Interconnected Power Systems in [6]. an attempt has been made to solve LFCs problem using grey wolf optimization (GWO) technique in two-area Interconnected Power Systems tacking into consideration GRC[7]. Imperialist competitive algorithm (ICA) was used to tune FOPID control parameters in linear two-area power systems[8]. LFC in a linear two-area power systems using the lévy-flight firefly optimization algorithm (LFOA) is presented in [9]. (FOPID) controller based on Gases Brownian Motion Optimization (GBMO) is used in order to mitigate frequency and exchanged power deviation in linear two-area power system in [10]. The development of a non-linear neural network controller using a generalized Hopfield neural network based self-adaptive PID controller has been investigated in [11]. Several robust control design techniques are used on the LFC problem so that the designed control unit is able to treat with system uncertainties. A Decentralized radial basis function neural network (RBFNN) based for LFC is used in three-area system [12], linear matrix inequalities (LMI) technique and iterative linear matrix inequalities (ILMI) algorithm are presented in [13], An adaptive Micro-Grid scheme including EV for LFC [14], optimal control theory and the linear quadratic regulator (LQR) is introduced in [15], LQR for a multi-area interconnected power system formulated and tested in[16]. There is numerous other widespread control strategies like

distributed economic model predictive control (DEMPC) strategy [17], the concept of active disturbance rejection control (ADRC) [18], singular value decomposition (SVD) in [19], etc. have also been used in decentralized LFC of multi-area power systems. This paper proposes a recently Mayfly Optimization (MOA) algorithm to tune the parameters of FOPID controllers in a nonlinear three-areas power system, as well as to comparatively study the proposed algorithm with GWO, ABC, and a recently Atom search optimization (ASO) introduced in[20], as well as compare the results with the last scenario in[21], where the GA algorithm is used to design PI controllers for the same system, but GA was unable to stabilize the system when all three constraints were enabled. Finally, the system was tested against parametric-uncertainties. The system simulation is recognized by using MatLab/Simulink.

II. FRACTIONAL-ORDER PID (FOPID) CONTROL

Thanks to its simple structure and functionality, integer-order PIDs (IOPIDs) are commonly used in industry. Such controller has the main gains that must tune appropriately in order to obtain good performance. Recently fractional calculus has emerged to generalize IO calculus. As a result fractional order PID controllers can simple parameterize all admissible PIDs, i.e. FOPID can characterize the whole set of controllers Including IOPIDs. From the design point of view, the parameters of the FOPID controller ($k_P, k_I, k_D, \lambda \; and \; \mu$) should be adjusted to enhance system performance. However IOPID controller has only the main gains(k_P, k_I, k_D). Summing up, FOPID can simply extend the search domain by integral and differential terms. Physically, exact implementing of fractional-order integral-deferential terms is not a straight forward process. Hence fractional terms are after approximated by rational functions of integer polynomials. Parallel FOPID controller block diagram is shown in Figure 1. various approximation based on exact frequency response of fractional terms are notable in control literature such as Crone, Carlson, , Oustaloup, Chareff approximation [22]and recently Modified Oustaloup approximation [23]. In this paper Oustaloup approximation is used. Oustaloup approximation is based on the approximation of a function of the form:

$$G(s) = s^{\alpha}, \alpha \in R^{+} \tag{1}$$

by rational function

$$\hat{G}(s) = C \prod_{k=1}^{N} \frac{1 + s/\acute{\omega}_k}{1 + s/\omega_k} \tag{2}$$

Using the following set of equations

$$\acute{\omega}_k = \omega_b \omega_u^{(2k-1-\alpha)/N}, \qquad \omega_k = \omega_b \omega_u^{(2k-1+\alpha)/N} \tag{3}$$

$$C = \omega_h^{\alpha}, \; \omega_u = \sqrt{\omega_h/\omega_b} \tag{4}$$

Where ω_h, ω_b are the high and low transitional frequencies.

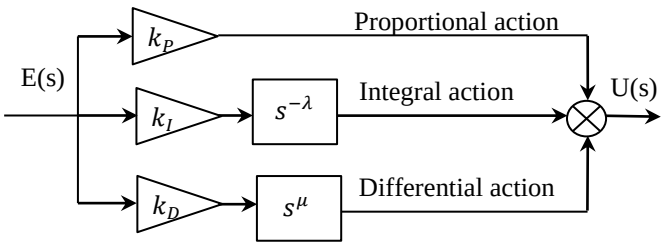

Figure 1 Parallel FOPID controller block diagram

III. MAYFLY OPTIMIZATION ALGORITHM

Mayflies are an ancient group of insects, which have more than 3000 species of it. After hatching from eggs they grow as aquatic nymphs. When mayflies reach adulthood, they ascend to the surface. An adult Mayfly lives only a few days, until it achieves its ultimate goal of reproduction. Adult males gather up in swarms, they perform nuptial dance to attract females. Females fly into these swarms to mate with males. When mating complete females drop their eggs to water. The mayfly optimization was first introduced by Zervoudakis, Tsafarakis[24]. The algorithm can be summarized as follows:

1. Initiation: initialize the population of males position as $x_i = [x_1, ..., x_d]$ and females $y_i = [y_1, ..., y_d]$ and its corresponding velocities $v_i = [v_1, ..., v_d]$.
2. Male movement: each mayfly adjusts its position toward its personal best position p_{best}, as well as the best position attained by its neighbors g_{best}. Which can be described as follows:

$$x_{ij}^{t+1} = x_{ij}^{t} + v_i^{t+1} \tag{5}$$

$$v_{ij}^{t+1} = v_{ij}^{t} + a_1 e^{-\beta r_p^2}\left(pbest_{ij} - x_{ij}^{t}\right) + a_2 e^{-\beta r_g^2}\left(gbest_{ij} - x_{ij}^{t}\right) \tag{6}$$

Where $x_{ij}^{t} \; and \; v_{ij}^{t}$ are the position and velocity of agent i at dimension j and iteration t. $a_1 \; and \; a_2$ are the global and personal learning coefficient .β is fixed coefficient. $r_p \; and \; r_g$ are personal and global Cartesian distance, respectively. The velocity of the best mayfly is given by $v_{ij}^{t+1} = v_{ij}^{t} + d * r$ .where r is random value in range of [-1, 1] and d is nuptial dance coefficient.

3. Female movement: female mayfly update its location according to the Cartesian distance between itself and males as follows:

$$y_{ij}^{t+1} = y_{ij}^{t} + v_i^{t+1} \tag{7}$$

$$v_{ij}^{t+1} = \begin{cases} v_{ij}^{t} + a_2 e^{-\beta r_{mf}^2}\left(x_{ij}^{t} - y_{ij}^{t}\right) \; if \; f(y_i) > f(x_i) \\ v_{ij}^{t} + fl * r \;\; if \;\; f(y_i) \le f(x_i) \end{cases} \tag{8}$$

Where $y_{ij}^{t} \; and \; v_{ij}^{t}$ are the position and velocity of female i at dimension j and iteration t. a_2 is a positive attraction coefficient .β is a fixed coefficient. r_{mf} is the Cartesian distance between female and male, respectively. fl is a random coefficient.

4. Mating of mayflies: male and female will mate and produce two off springs. Which equation as follows:

$$offspring\ 1 = L * male + (1 - L) * female$$
$$offspring\ 2 = L * female + (1 - L) * male \tag{9}$$

Where L is random number, male is a male parent and female is female parent. One off spring will be added to male population and the other off spring will be added to female population. Off spring initial velocities will be equal to zeros. The select of male and female can be random or based on fitness.

5. Update solutions: worst solutions are replaced with the best new ones, then gbest, pbest will be updated. The

above steps repeated until stop criteria is met.

IV. CASE STUDY

The single line diagram of the proposed system is shown in Figure 2. Every area contains FOPID controller, governor and a single reheat turbine .GRC, Time delay and dead band physical constrains are considered together in this system, where GRC is equal to 3% p.u.MV/min, time delay is 2 seconds and dead band is 0.036 Hz. Areas are connected via a power line called the tie line. ACE signal is filtered before being used by low-pass filter with a corner frequency Fc=5 Hz, a 0.02 p.u. system is stimulated with step load perturbation (SLP) applied to areas 1 and 3. System parameters are shown in appendix A and these parameters are taken from [25] .The dynamic model of three-area power system is shown in Figure 3.

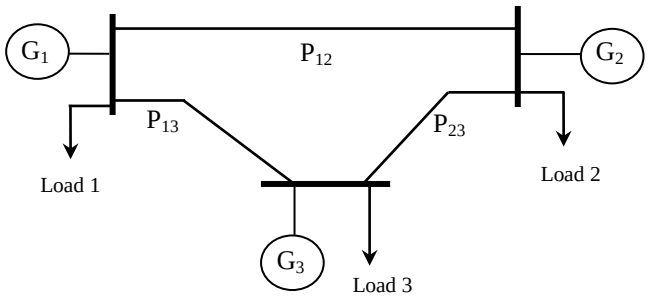

Figure 2 Single line diagram of the suggested three-area test system.

V. SIMULATION RESULTS AND EVALUATION

Four different meta-heuristic optimization techniques (MOA,GWO,ABC and ASO) have been proposed in this paper to optimally tune the suggested FOPID controllers in each of the three-areas. Each algorithm is executed for 100 iterations. The perfomance measure used in this paper is integral time weighted absolute error (ITAE) index, which is used to minimize the error in both of frequency and tie line power. ITAE punishes long duration transients, and it gives better results for this system. A system designed using this criterion shows well damped oscillations and minimal overshoots. ITAE is defined as:

$$ITAE = \int_0^{t_{sim}} t|\Delta f_1 + \Delta f_2 + \Delta f_3 + \Delta p_{12} + \Delta p_{23} + \Delta p_{13}| \quad (10)$$

where t_{sim} is simulation time. GA based PI controller results in [21] have been also considered in simulation results. Table 1 simply presents optimal parameters of fractional PID controllers deduced / computed by MOA, GWO, ABC, and ASO. The performance index for performed algorithms is shown in Table 2. It is obvious from Table 2 that MOA have the best ITAE cost function. Fitness function of MOA, GWO, ABC, and ASO is shown in Figure 4. The MOA exhibits good convergence which becomes the best after 27 epochs. A set of time domain specification is given in Table 3 using different algorithms. Clearly MOA-based FOPID controllers result in minimum settling time of about 14 sec in area-1 while all algorithms give equal frequency undershooting. From the frequency response in Figure 5 and the Tie-line power response in Figure 6 it is obvious that the GA-based PI controller system failed to stabilize the system. Figure 7 shows the generation rate and, as can be seen, GA reaches the saturation limit but the other algorithms are far from reaching this limit. Control signal effort in Table 4 shows that MOA have the highest control effort. It can be concluded that the MOA algorithm based controller enhance the dynamic performance of the system as compare to the other algorithms.

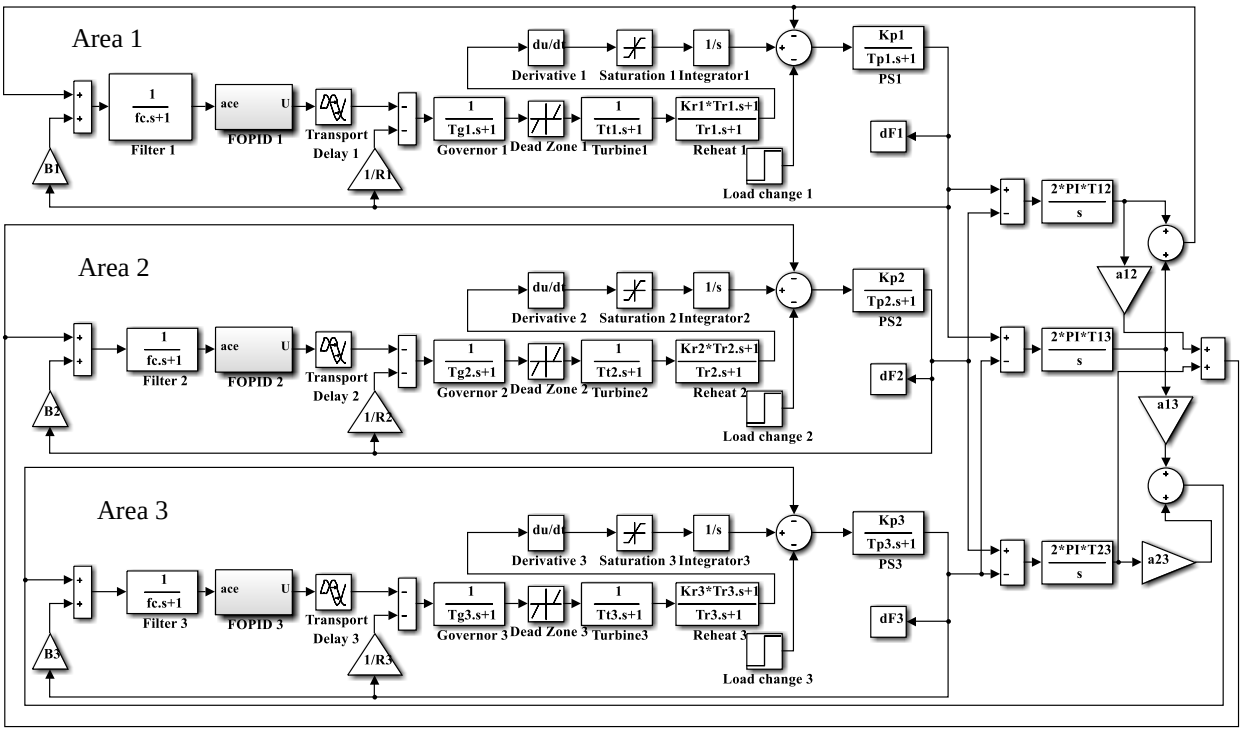

Figure 3 Nonlinear three –area thermal power system considering GRC, TD, and DB.

Table 1 Optimum values of FOPID parameters by MOA, GWO, ABC, and ASO.

		k_p	k_i	λ	k_d	μ
Area 1	MOA	1	0.15027	0.00002	0.00749	1.89035
	GWO	1.0	0.14982	0.00012	0.28877	0.00375
	ABC	0.98174	0.12841	0.01398	0.28849	0.10325
	ASO	0.80867	0.12173	0.11262	0.31119	0.46511
Area 2	MOA	0.99994	0.14528	0.05284	0.74014	0.00007
	GWO	1.0	0.08236	0.12046	0.34294	0.08490
	ABC	1.0	0.20012	0	1.0	0
	ASO	0.53672	0.07327	0.1282	0.54321	0.71907
Area 3	MOA	0.9939	0.15344	0	0.39246	0
	GWO	1.0	0.08236	0.12046	0.34294	0.08490
	ABC	0.90787	0.17652	0	0.06689	1.7996
	ASO	0.59508	0.11102	0.00006	0.6596	0.40405

Table 2 ITAE cost function computed by MOA, GWO, ABC, and ASO.

Algorithm	MOA	GWO	ABC	ASO
ITAE	17.66	19.115	22.115	54.052

Table 3 Settling time, settling maximum, settling minimum, peak time and peak values of the frequency response.

Area	algorithm	t_s second	Δf^+ Hz	Δf^- Hz	T_p second	Δf_{max} Hz
1	MOA	13.993	0.00456	-0.0035	4.2508	0.1727
	GWO	22.143	0.0077	-0.1733	4.2486	0.1733
	ABC	19.734	0.008	-0.0013	4.2759	0.17484
	ASO	48.375	0.0156	-0.1708	4.265	0.1708
2	MOA	16.24	0.00507	-0.0052	3.658	0.1785
	GWO	22.817	0.0078	-0.0049	3.669	0.1787
	ABC	19.108	0.0073	-0.1783	3.6582	0.17828
	ASO	49.146	0.0185	-0.0182	3.658	0.17876
3	MOA	19.273	0.00568	-0.0077	4.3492	0.17049
	GWO	23.691	0.0081	-0.0044	4.3438	0.1705
	ABC	18.249	0.0069	-0.0056	4.299	0.17037
	ASO	49.915	0.01741	-0.1707	4.339	0.17067

Table 4
Control signal effort

	Area 1				Area 2				Area 3			
Algorithm	MOA	GWO	ABC	ASO	MOA	GWO	ABC	ASO	MOA	GWO	ABC	ASO
$\|\|u_i\|\|_2$	6.1264	3.0501	6.1856	4.1854	3.4309	1.4138	3.3498	2.035	6.1213	3.0482	6.3546	3.9539

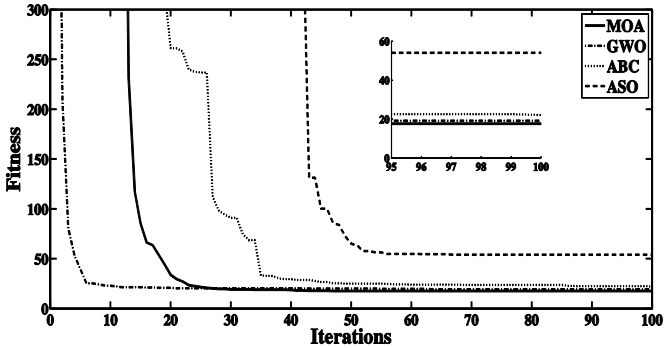

Figure 4 Fitness and iterations curve

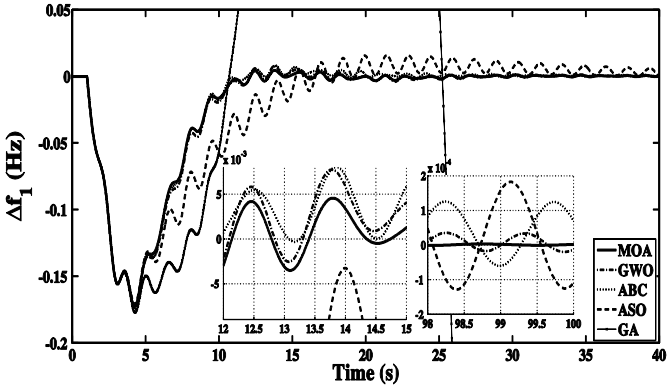

(a)

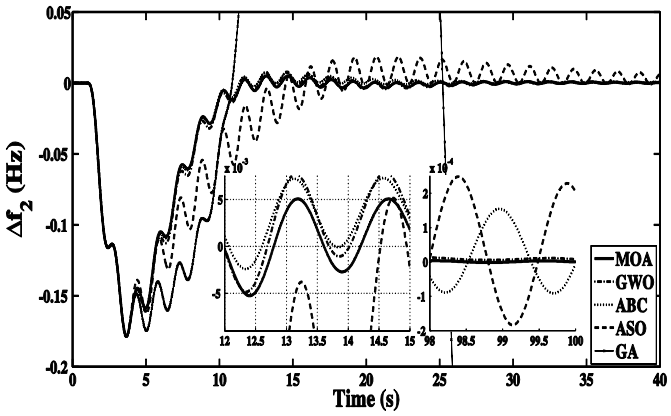

(b)

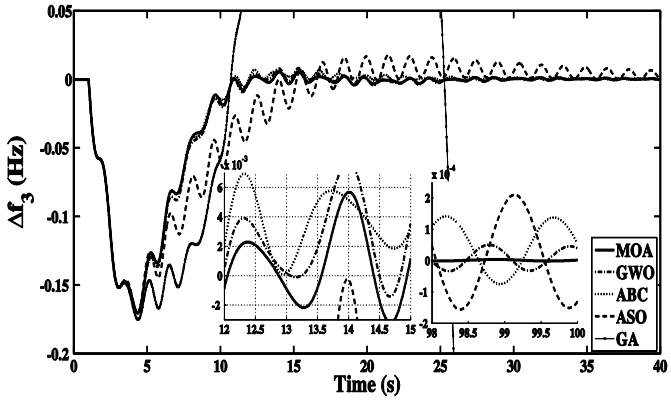

(c)

Figure 5 Frequency response for: (a) Area 1,(b) Area 2 and (c) Area 3.

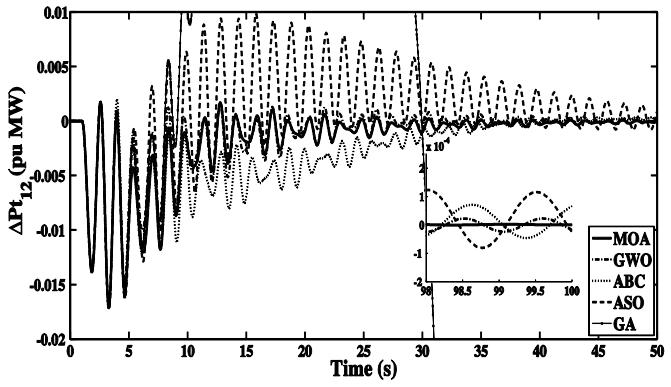

(a)

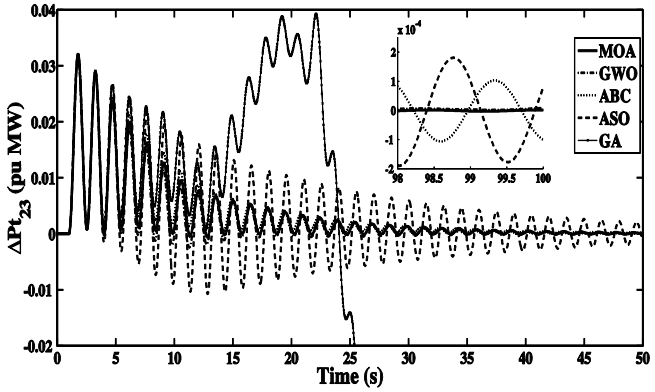

(b)

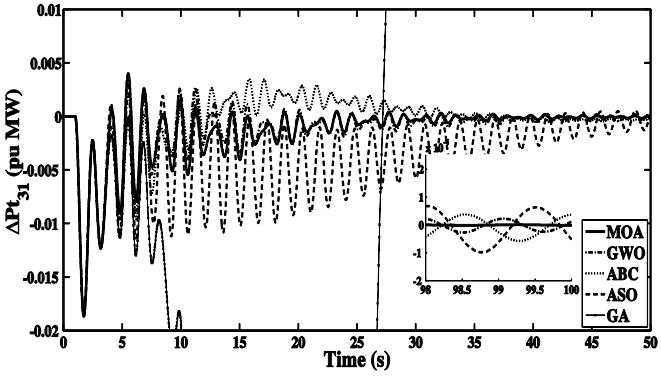

(c)

Figure 6 Tie-line power response for: (a) Area 1,(b) Area 2 and (c) Area 3.

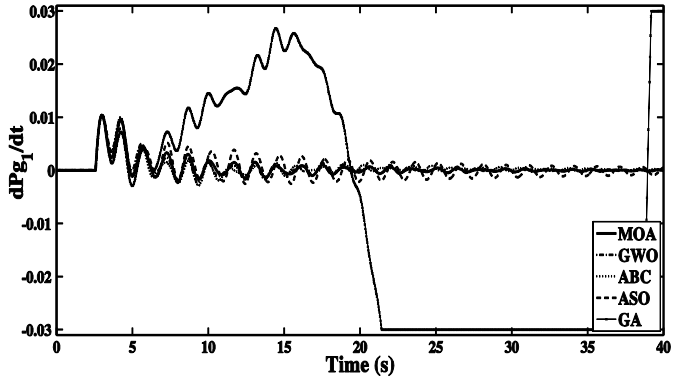

(a)

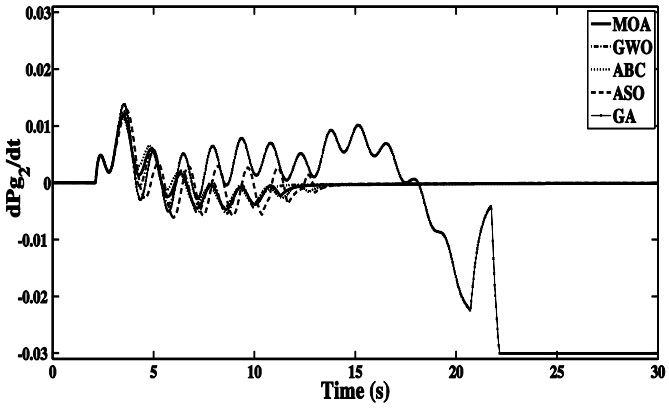

(b)

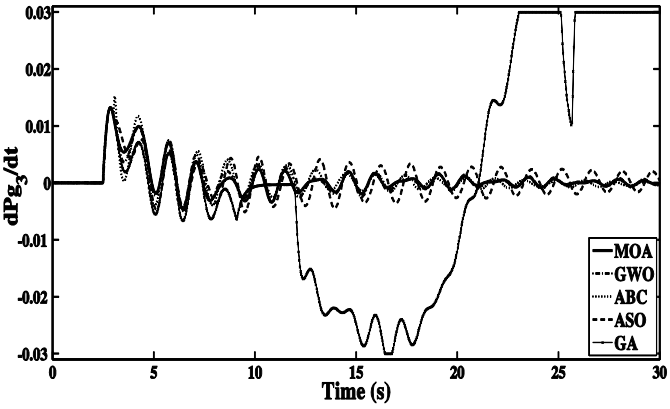

(c)

Figure 7 generation rate deviation for: (a) Area 1,(b) Area 2 and (c) Area 3.

VI. ROBUSTNESS TEST USING HERMITE-BIEHLER THEOREM

Hermite-Biehler theorem is used to test robustness of the system against parametric-uncertainties. This theorem states that a given real polynomial must satisfy a certain interlacing property to be Hurwitz stable. A real polynomial of degree n can be written as:

$$\delta(s) = \delta_0 + \delta_1 s + \cdots + \delta_n s^n \quad (11)$$

This can be arranged as:

$$\delta(s) = \delta_e(s^2) + s\delta_o(s^2) \quad (12)$$

Where δ_e, δ_o are the coefficients of the even and odd powers of s respectively. Then $\delta(s)$ is Hurwitz stable when the non-negative real zeros of $\delta_e(-\omega^2)\ and\ \delta_o(-\omega^2)$ satisfy the following interlacing property:

$$0 < \omega_{e1} < \omega_{o1} < \omega_{e2} < \omega_{o2} < \cdots \quad (13)$$

For the system under discussion, a robustness test is created with an error of ± 10% in the system parameters. Changing the system parameters in the specified range will result in several values for each of the even and odd frequency bands. The minimum and maximum values of the frequency bands of the system polynomial are shown in Table 5. By observing the results shown in Table 5, no intersection between periods was found and the interlacing property was satisfied.

Table 5 Odd/even frequencies interlocking of the system polynomial.

i	ω_{ei}		ω_{oi}		i	ω_{ei}		ω_{oi}	
	Min	Max	Min	Max		Min	Max	Min	Max
1	0.00898	0.009	0.018	0.019	11	4.061	4.084	4.144	4.212
2	0.029	0.03	0.041	0.043	12	4.872	5.155	5.345	5.369
3	0.055	0.058	0.073	0.077	13	5.461	5.61	6.691	7.245
4	0.096	0.102	0.126	0.133	14	8.845	9.547	11.57	12.42
5	0.164	0.173	0.217	0.228	15	14.97	15.97	19.25	20.39
6	0.287	0.301	0.382	0.4	16	24.73	26.03	31.92	33.38
7	0.508	0.532	0.672	0.704	17	41.57	43.18	54.72	56.47
8	0.884	0.929	1.158	1.226	18	72.94	74.82	98.85	100.9
9	1.52	1.622	2.008	2.161	19	137.88	140.2	203.16	206
10	2.672	2.894	3.556	3.813	20	334.31	338.22	721.8	728.8

VII. CONCLOSION

In this work FOPID is tuned by MOA algorithm and is established for LFC for three area systems tacking into consideration non linarites GRC, DB and TD. By considering these constrains the dynamic behavior of interconnected power system are more realistic. These constrains have strong impact in the system and make the system severely nonlinear as a result, adjusting the controller parameters may not be an easy task. After comparing simulation results it can be concluded that FOPID tuned by MOA provides better performance than the other discussed controllers. The controller has achieved good performance for both of frequency and tie-line power exchange, as well as tolerance to parameters deviations with a predetermined limit.

Appendix A.

$D_1 = D_3 = 0.015$, $D_2 = 0.016$ [p.u./Hz]; $2H_1 = 0.1667$, $2H_2 = 0.2017$, $2H_3 = 0.1247$ [s]; $R_1 = 3$, $R_2 = 2.73$,$R_3 = 2.82$ [Hz/p.u.]; $T_{g1} = 0.08$, $T_{g2} = 0.06$, $T_{g3} = 0.07$ [s]; $T_{t1} = 0.4$, $T_{t2} = 0.44$, $T_{t3} = 0.3$ [s];$B_1 = 0.3483$, $B_2 = 0.3827$, $B_3 = 0.3692$ [p.u./Hz]; $T_{12} = 0.2$, $T_{13} = 0.25$, $T_{23} = 0.12$ [p.u./Hz]; $k_{r1} = k_{r2} = k_{r3} = 0.5$; $T_{r1} = T_{r2} = T_{r3} = 10$ [s].

REFERENCES

[1] A. M. Mosaad, M. A. Attia, and A. Y. Abdelaziz, "Whale optimization algorithm to tune PID and PIDA controllers on AVR system," *Ain Shams Eng. J.*, vol. 10, no. 4, pp. 755–767, 2019, doi: 10.1016/j.asej.2019.07.004.

[2] K. Vrdoljak, N. Perić, and I. Petrović, "Sliding mode based load-frequency control in power systems," *Electr. Power Syst. Res.*, vol. 80, no. 5, pp. 514–527, 2010, doi: 10.1016/j.epsr.2009.10.026.

[3] S. Prasad, S. Purwar, and N. Kishor, "Load frequency regulation using observer based non-linear sliding mode control," *Int. J. Electr. Power Energy Syst.*, vol. 104, no. June 2018, pp. 178–193, 2019, doi: 10.1016/j.ijepes.2018.06.035.

[4] R. Kumar, S. Panda, and P. Chandra, "Electrical Power and Energy Systems Design and analysis of hybrid firefly algorithm-pattern search based fuzzy PID controller for LFC of multi area power systems," *Int. J. Electr. POWER ENERGY Syst.*, vol. 69, pp. 200–212, 2015, doi: 10.1016/j.ijepes.2015.01.019.

[5] R. Umrao, S. Kumar, M. Mohan, and D. K. Chaturvedi, "Load Frequency Control methodologies for power system," *ICPCES 2012 - 2012 2nd Int. Conf. Power, Control Embed. Syst.*, 2012, doi: 10.1109/ICPCES.2012.6508133.

[6] N. El, Y. Kouba, M. Menaa, M. Hasni, and M. Boudour, "Optimal Load Frequency Control Based on Artificial Bee Colony Optimization Applied to Single , Two and Multi - Area Interconnected Power Systems," 2015, [Online]. Available: https://ieeexplore.ieee.org/document/7233027?arnumber=7233027.

[7] D. Guha, P. K. Roy, and S. Banerjee, "Load frequency control of interconnected power system using grey Wolf optimization," *Swarm Evol. Comput.*, vol. 27, pp. 97–115, 2016, doi: 10.1016/j.swevo.2015.10.004.

[8] S. A. Taher, M. Hajiakbari Fini, and S. Falahati Aliabadi, "Fractional order PID controller design for LFC in electric power systems using imperialist competitive algorithm," *Ain Shams Eng. J.*, 2014, doi: 10.1016/j.asej.2013.07.006.

[9] M. R. Shakarami, I. Faraji, I. Asghari, and M. Akbari, "Optimal PID tuning for load frequency control using lévy-flight firefly algorithm," *2013 3rd Int. Conf. Electr. Power Energy Convers. Syst. EPECS 2013*, pp. 2–6, 2013, doi: 10.1109/EPECS.2013.6713008.

[10] A. Zamani, S. M. Barakati, and S. Yousofi-Darmian, "Design of a fractional order PID controller using GBMO algorithm for load–frequency control with governor saturation consideration," *ISA Trans.*, vol. 64, pp. 56–66, 2016, doi: 10.1016/j.isatra.2016.04.021.

[11] R. Ramachandran, B. Madasamy, V. Veerasamy, and L. Saravanan, "Load frequency control of a dynamic interconnected power system using generalised Hopfield neural network based self-adaptive PID controller," *IET Gener. Transm. Distrib.*, vol. 12, no. 21, pp. 5713–5722, 2018, doi: 10.1049/iet-gtd.2018.5622.

[12] H. Shayeghi, H. A. Shayanfar, and O. P. Malik, "Robust decentralized neural networks based LFC in a deregulated power system," *Electr. Power Syst. Res.*, vol. 77, no. 3–4, pp. 241–251, 2007, doi: 10.1016/j.epsr.2006.03.002.

[13] H. Bevrani and T. Hiyama, "Robust decentralised PI based LFC design for time delay power systems," *Energy Convers. Manag.*, vol. 49, no. 2, pp. 193–204, 2008, doi: 10.1016/j.enconman.2007.06.021.

[14] M. Khooban, T. Niknam, F. Blaabjerg, and P. Davari, "A robust adaptive load frequency control for micro-grids," *ISA Trans.*, pp. 1–10, 2016, doi: 10.1016/j.isatra.2016.07.002.

[15] E. Lavretsky and K. A. Wise, "Optimal control and the linear quadratic regulator," *Adv. Textb. Control Signal Process.*, no. 9781447143956, pp. 27–50, 2013, doi: 10.1007/978-1-4471-4396-3_2.

[16] A. P. Huddar and P. S. Kulkarni, "Load frequency control of a multi-area power system using linear quadratic regulator," *J. Inst. Eng. Electr. Eng. Div.*, vol. 90, no. JUNE, pp. 28–32, 2009.

[17] C. Zhang, S. Wang, and Q. Zhao, "Distributed economic MPC for LFC of multi-area power system with wind power plants in power market environment," *Int. J. Electr. Power Energy Syst.*, vol. 126, no. PB, p. 106548, 2021, doi: 10.1016/j.ijepes.2020.106548.

[18] L. Dong, Y. Zhang, and Z. Gao, "A robust decentralized load frequency controller for interconnected power systems," *ISA Trans.*, vol. 51, no. 3, pp. 410–419, 2012, doi: 10.1016/j.isatra.2012.02.004.

[19] G. Ray, A. N. Prasad, and T. K. Bhattacharyya, "Design of decentralized robust load-frequency controller based on SVD method," *Comput. Electr. Eng.*, vol. 25, no. 6, pp. 477–492, 1999, doi: 10.1016/S0045-7906(99)00020-8.

[20] W. Zhao, L. Wang, and Z. Zhang, "A Novel Atom Search Optimization for Dispersion Coefficient Estimation in Groundwater," *Futur. Gener. Comput. Syst.*, 2018, doi: 10.1016/j.future.2018.05.037.

[21] H. Golpîra, H. Bevrani, and H. Golpîra, "Application of GA optimization for automatic generation control design in an interconnected power system," *Energy Convers. Manag.*, vol. 52, no. 5, pp. 2247–2255, 2011, doi: 10.1016/j.enconman.2011.01.010.

[22] I. Podlubny, I. Petráš, B. M. Vinagre, P. O'Leary, and L. Dorčák, "Analogue realizations of fractional-order controllers," *Nonlinear Dyn.*, vol. 29, no. 1–4, pp. 281–296, 2002, doi: 10.1023/A:1016556604320.

[23] C. A. Monje, Y. Chen, B. M. Vinagre, D. Xue, and V. Feliu, *Fractional Order Systems and Controls*. 2010.

[24] K. Zervoudakis and S. Tsafarakis, *A mayfly optimization algorithm Stelios Tsafarakis , PhD*. Elsevier Ltd, 2020.

[25] H. Bevrani, *Robust Power System Frequency Control (Power Electronics and Power Systems)*. 2009.